A Summary of the DRAGRACER Flight Experiment for Orbital Debris Mitigation and Radiometric Solutions

Patrick Kelly, PhD; Ellen Glad
Millennium Space Systems, A Boeing Company

ABSTRACT

DRAGRACER was a 2020 flight demonstration mission to characterize the orbital debris mitigation properties of deployable tethers as well as to validate ground observability of commercial-off-the-shelf (COTS) LEDs on-orbit. The scientific-method-based deorbit study was executed using two nearly identical modules that were deployed simultaneously into a 500 km, sun-synchronous orbit. One module was equipped with a 70-meter-long tether while the other served as a control unit to provide a one-to-one basis for deorbit comparison. The tethered module deorbited within 8 months while the other will remain on orbit for over a decade. Both satellites were observed using COTS ground equipment, confirming observability of the LEDs. This paper summarizes the findings of the DRAGRACER flight experiment, including insights into orbital decay rates, drag estimation parameters, and a radiometric study analyzing the observability of COTS LEDs on-orbit.

1. INTRODUCTION

The primary purpose of the DRAGRACER mission was to characterize the performance of space tethers as a viable means of orbital debris mitigation using a scientific-method-based approach. Millennium achieved this through observation and comparison of each satellite's orbit and orbit histories. ALCHEMY provided the experimental information while AUGURY served as the control unit, providing a baseline for comparison. The DRAGRACER mission additionally provided insight into the observability of COTS LEDs and the highly reflective tether.

Radar measurements for the DRAGRACER satellites were first observed on 20 November 2020 from space-track.org. ALCHEMY was first designated OBJECT AB with NORAD catalog ID 46954. AUGURY was first designated OB-JECT AC with NORAD catalog ID 46955. After successful electro-optical observation of both flight vehicles on 01 December 2020, the 18th Space Control Squadron (SPCS) was notified and ALCHEMY and AUGURY were officially identified. Sunlit images of both flight units were recorded on the morning of 13 June 2021 from Joshua Tree, CA. On 19 July 2021, the final measurements of ALCHEMY were recorded shortly before it's reentry event. AUGURY is not expected to deorbit for approximately 15 more years. Major technical milestones are summarized in Table 1

Table 1: DRAGRACER Key Technical Milestones

Milestone	Date
Launch	2020 November 20
First Radar Measurements	2020 November 20
First Images Collected	2020 December 01
Satellite IDs Confirmed	2020 December 01
Sunlit Images Collected	2021 June 13
ALCHEMY Reentry	2021 July 19
AUGURY Reentry	2037 Spring (est.)

Copyright © 2023 Advanced Maui Optical and Space Surveillance Technologies Conference (AMOS) – www.amostech.com

2. FLIGHT EXPERIMENT

ALCHEMY and AUGURY were constructed with identical stowed mass properties and dimensions. When stacked in their launch configuration, DRAGRACER creates a composite 12U form-factor as illustrated in Fig. 1. These satellites were launched, simultaneously, into a common low-Earth orbit. ALCHEMY deployed a space tether while AUGURY served as a scientific control unit to provide the baseline for comparison. Both orbits were recorded for the duration of one year and their resulting deorbit profiles were compared.

Fig. 1: DRAGRACER stowed configuration.

DRAGRACER launched on a Rocket Lab Electron launch vehicle which launched from Mahia, NZ on 20 November 2020 at 02:20 UTC. Both vehicles were inserted into a sun-synchronous, 500 km orbit. Space-Track cataloged the objects for their SATCAT database within the first 24 hours of launch and the DRAGRACER vehicles would eventually be identified as 46954 DRAGRACER1(ALCHEMY) and 46955 DRAGRACER2(AUGURY).

2.1 Data

Orbital data for the flight experiment was collected primarily from Space-Track.org. Full element sets were collected for each spacecraft and were downloaded as .json files. A summary of the orbit profiles for each DRAGRACER vehicle is provided in Fig. 2. It is clear from the data that the two satellites experienced vastly different deorbit profiles over the 1 year investigation. ALCHEMY deorbited in approximately 8 months, while AUGURY's altitude seems virtually unchanged. The semimajor axis profile immediately illustrates the qualitative differences in the orbit sizes over time. The size of the ALCHEMY orbit shrinks at a more rapid pace due to the drag tether. Examination of the eccentricity profiles for each satellite suggests that the orbits are near circular for the entirety of the flight experiment. This is expected as atmospheric drag tends to circularize LEO orbits and dampen eccentricity growth from other perturbing forces. With low eccentricities confirmed for each satellite, circular orbit approximations are reasonable for the orbit analysis activities in Section 2.2. The inclination for both orbits were largely unchanged, as both remained within 0.1° of their original sun-synchronous inclination. The right ascension of the ascending node drifted similarly for both satellites due to Earth's $J2$ effect. Their drift rates were very similar due to their near-identical inclinations throughout the experiment. The argument of perigee behavior followed a mostly similar drifting trend for both satellites, also due in large part to Earth's $J2$ effect. The sudden jump in the ALCHEMY ω profile coincides with a sharp decrease in eccentricity in late May. As $e \to 0$, it is not uncommon for ω histories to become erratic as the perigee vector is constantly redefined. The true anomaly profile is included to further illustrate the uniform sampling of measurements throughout the flight experiment.

To assist with data analysis tasks, space weather data was collected for the duration of the flight experiment. Specifically, solar activity and magnetic indices were collected to provide more accurate approximations of the atmospheric density profiles experienced by the DRAGRACER spacecraft. These values were obtained via CelesTrak's public space weather database. Figure 3 provides a snapshot of the solar activity during the DRAGRACER flight experiment.

Copyright © 2023 Advanced Maui Optical and Space Surveillance Technologies Conference (AMOS) – www.amostech.com

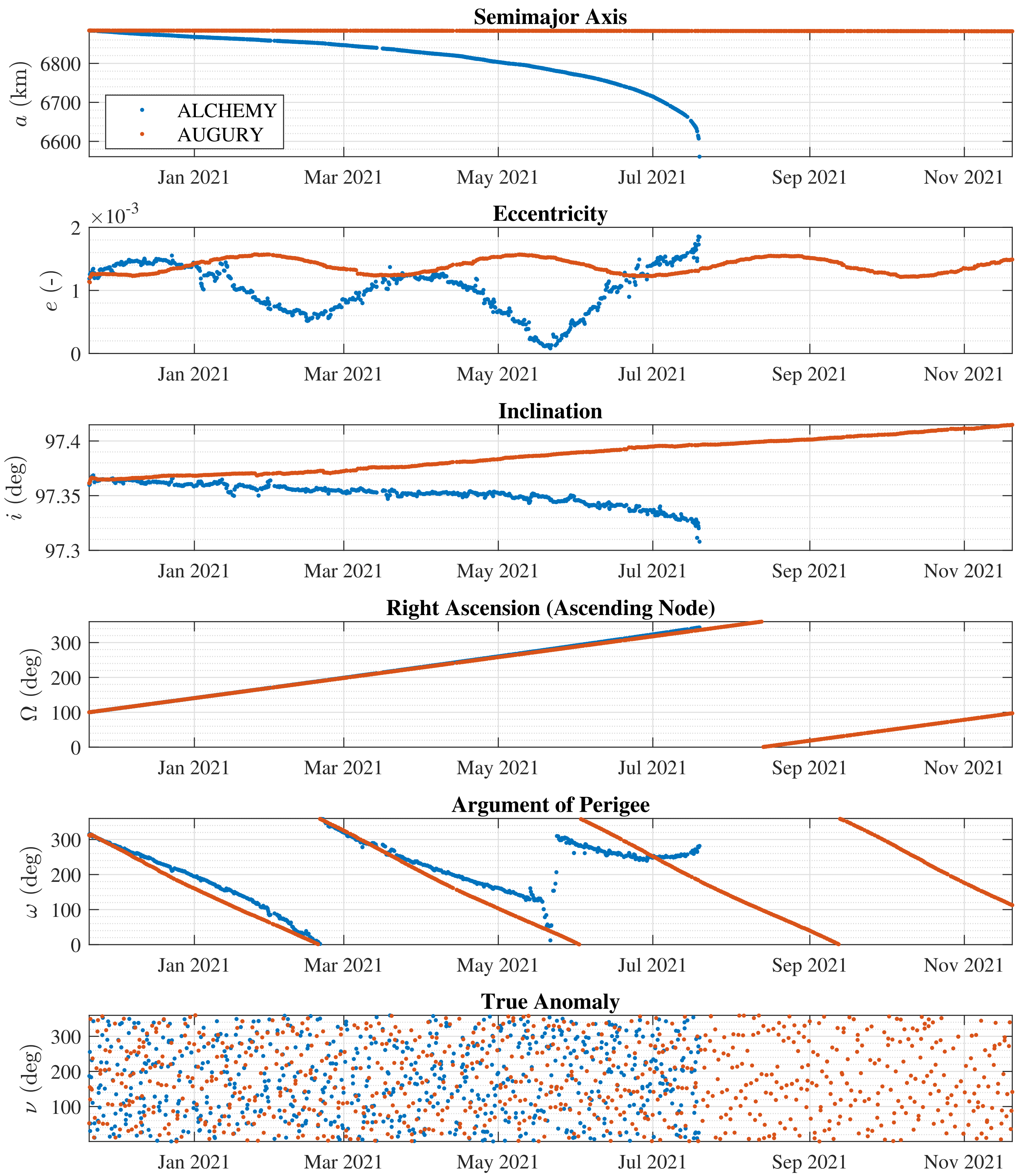

Fig. 2: Orbit comparison of DRAGRACER flight units.

Copyright © 2023 Advanced Maui Optical and Space Surveillance Technologies Conference (AMOS) – www.amostech.com

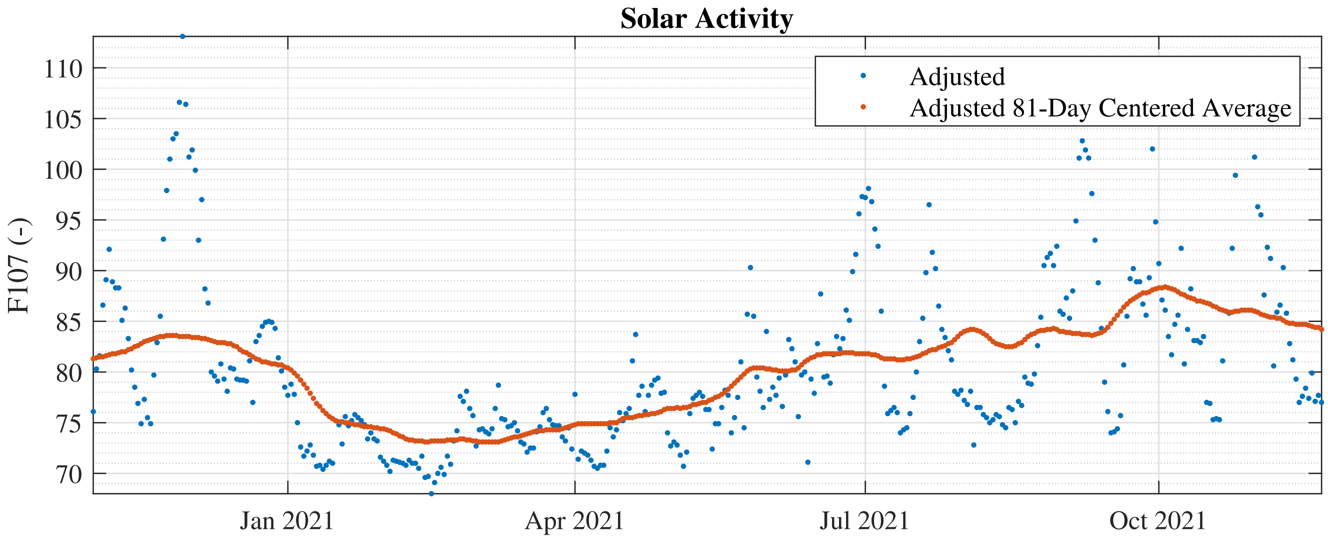

Fig. 3: Solar activity summary during the DRAGRACER flight experiment.

2.2 Analysis

2.2.1 Altitude and Decay Rates

Data from the Space-Track.org ELSETs provides mean elements for each spacecraft. Since the semimajor axis is reported directly from this data set, the altitude (h) history is readily obtained using

$$h \approx a - R_{\oplus} \tag{1}$$

where $R_{\oplus}$ is the mean Earth radius. Equation (1) is deemed valid due to the circular orbit approximation. The DRAGRACER altitude summary is provided in Fig. 4. It is clear from the data that the two satellites experienced vastly different deorbit profiles over the one year investigation. ALCHEMY deorbited in approximately 8 months, while AUGURY's altitude seems virtually unchanged, having decayed only $\sim$ 1.85 km over one year.

Mean decay rates are reasonably obtained using the following approximation

$$\dot{a} \approx \frac{\Delta a}{\Delta t} \tag{2}$$

The majority of the satellite's orbit is characterized by a relatively small Δa over a small interval Δt. With Δt durations on the order of hours across the duration of the experiment, Eq. (2) is also a reasonable approximation of the instantaneous decay rate. The DRAGRACER decay rate summaries are provided in Fig. 5.

Copyright © 2023 Advanced Maui Optical and Space Surveillance Technologies Conference (AMOS) – www.amostech.com

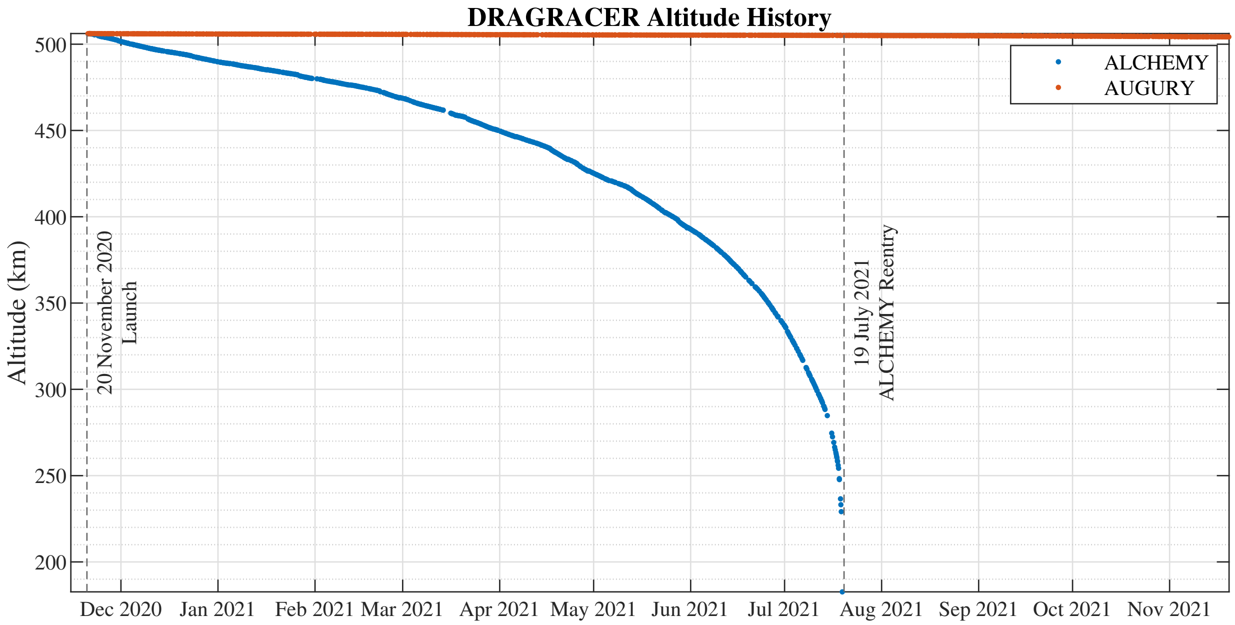

Fig. 4: DRAGRACER deorbit profile over 1 year. ALCHEMY remained on-orbit for approximately 8 months. AUGURY is expected to remain on orbit for approximately 15 years or longer.

2.2.2 Drag Estimation Parameters

For an object in near circular orbit, the specific drag force can be approximated using

$$F_D \approx \frac{n\dot{a}}{2} \tag{3}$$

where F_D is the specific drag force, n is the mean motion, and $\dot{a}$ is the time rate of change in semimajor axis. Using the $\dot{a}$ approximations from Section 2.2.1, and n from the ELSETs, the drag force is readily obtained. Figure 6 illustrates the specific drag force as a function of altitude. The atmospheric density can be obtained using historic space weather data from CelesTrak in conjunction with each satellite's reported state history. Inserting environmental and state information into an NRLMSISE00 model, the atmospheric density history for each DRAGRACER vehicle is obtained. DRAGRACER atmospheric density histories are provided in Fig.7.

The ballistic coefficient, BC, can be obtained using

$$BC = -\frac{n\dot{a}}{\rho v_{\text{rel}}^2} \tag{4}$$

where ρ is atmospheric density and v_{rel} is the relative velocity of the satellite with respect to the Earth's atmosphere. Solving for BC using Eq. (4) yields ballistic coefficient histories illustrated in Fig. 8

The effective drag area can be obtained using the assumed $C_D = 2.2$ and known satellite masses as illustrated in Fig. 9 Estimated drag parameters for the DRAGRACER satellites are summarized in Table 2.

Table 2: Estimated Drag Parameters for DRAGRACER Orbits

Module	Area	Ballistic Coefficient
ALCHEMY	1.832 m^2	0.3403 $\frac{m^2}{kg}$
AUGURY	0.045 m^2	0.0085 $\frac{m^2}{kg}$

Copyright © 2023 Advanced Maui Optical and Space Surveillance Technologies Conference (AMOS) – www.amostech.com

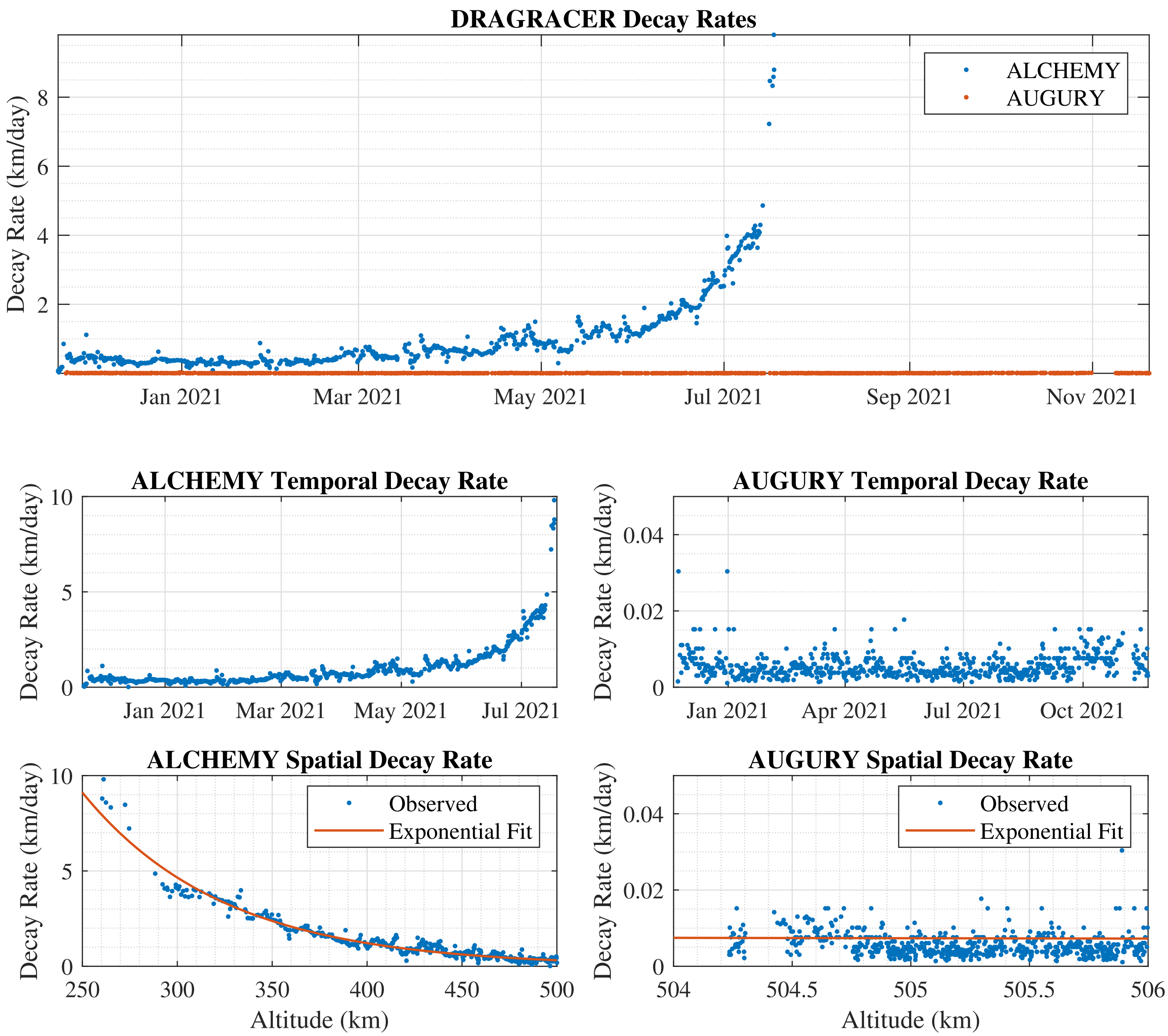

Fig. 5: DRAGRACER decay rates by time and altitude.

Copyright © 2023 Advanced Maui Optical and Space Surveillance Technologies Conference (AMOS) – www.amostech.com

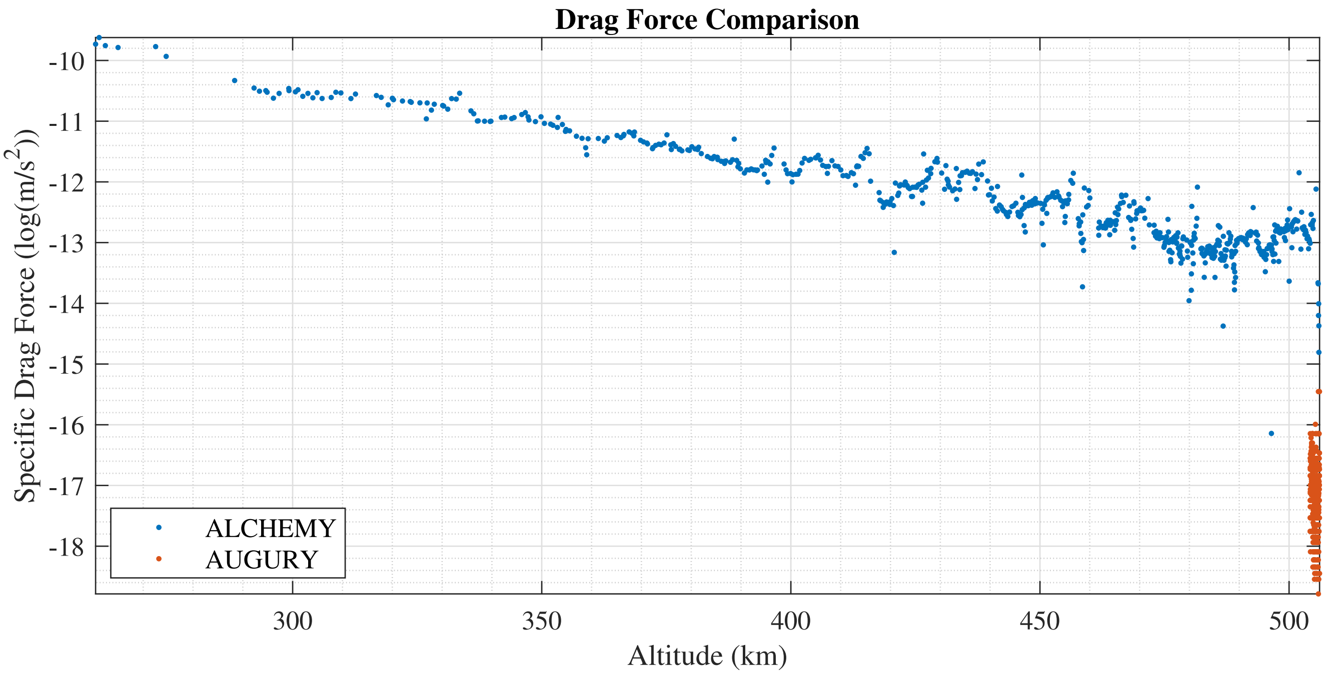

Fig. 6: Specific drag force experienced by the DRAGRACER flight units as a function of altitude.

2.3 Deorbit Analysis Conclusions

The DRAGRACER flight experiment proved that space tether technology is indeed a viable means of low-complexity, accelerated deorbit. As predicted, ALCHEMY experienced a significant reduction in orbit lifetime, with a total of 8 months on-orbit. Based on work-energy principle approximations, AUGURY is expected to deorbit after 26.70 years as ALCHEMY's *BC* was 40.27 times greater on average. This serves as an upper bound as the DRAGRACER flight experiment took place during a minimum in the solar cycle. AUGURY's expected atmospheric density profile is expected to increase by an order of magnitude during the solar max season. The STK lifetime tool estimates a lifetime of 14.9 years using the NRLMSISE00 density model and a lifetime of 59 years using SGP4 propagation. Based on these estimates it is reasonable to assume AUGURY's reentry date will likely fall between 14.9 and 26.7 years.

Assuming a satellite's probability of on-orbit collision (P_C) is proportionate to the area-time product (ATP) such that $P_C \propto A \cdot \Delta t$, ALCHEMY experienced a total ATP of 441.5120 m^2day. This is approximately the same expected ATP for AUGURY due to the work-energy principle. In terms of calculating the high-energy collision risk, we must account for the 1.832 m^2 tether area. Removing this area from ALCHEMY's ATP calculation, we arrive at an updated value of 13.4237 m^2day. The total high-energy collision risk using a tether-assisted deorbit was reduced by 96% for ALCHEMY. These values are summarized in Table 3

Table 3: High-energy collision area time products for DRAGRACER flight experiment.

Area Time Product (m^2day)	
Nominal	Tether-Assisted
441.5210	13.4237

Copyright © 2023 Advanced Maui Optical and Space Surveillance Technologies Conference (AMOS) – www.amostech.com

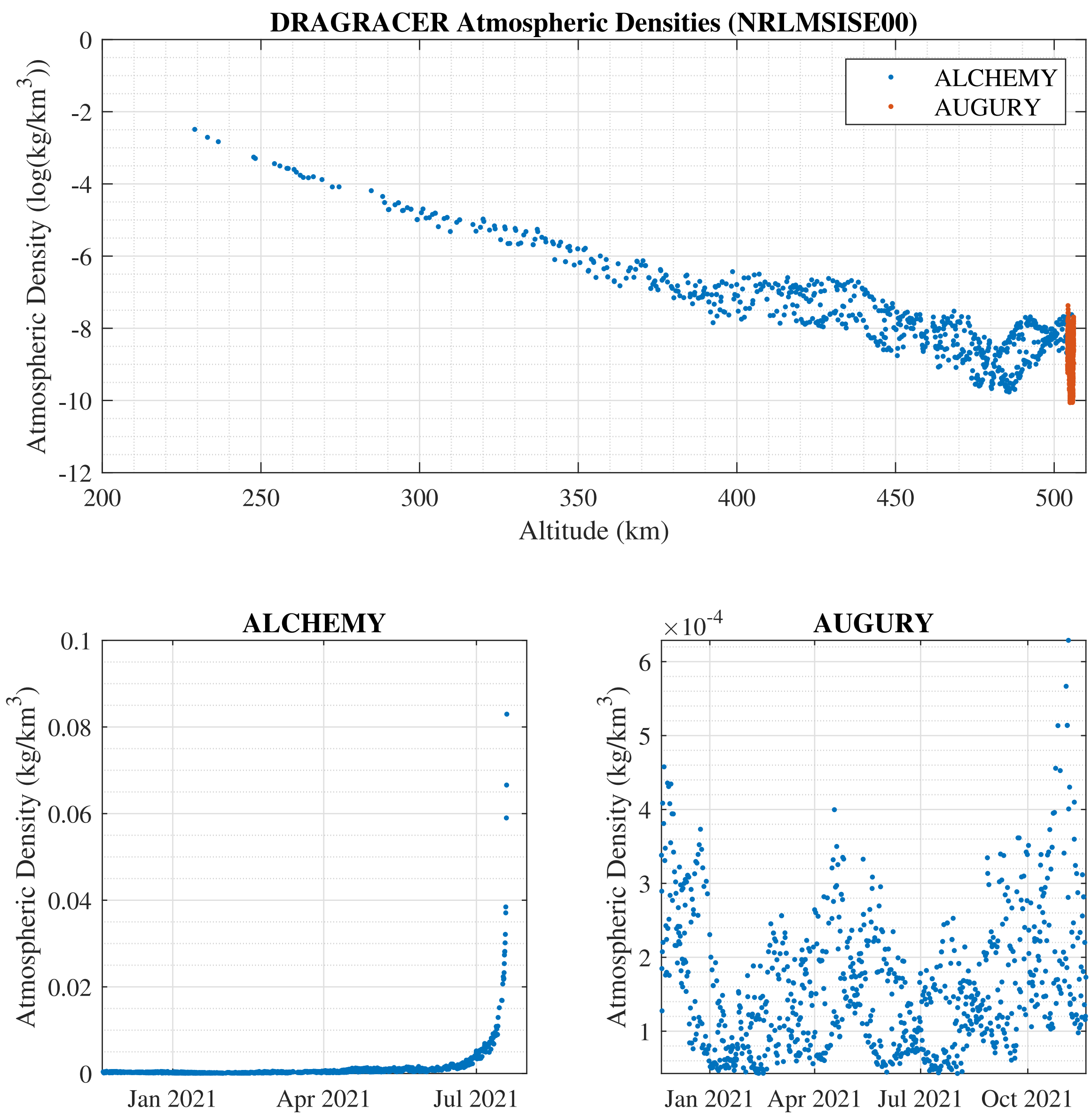

Fig. 7: Atmospheric density profiles for DRAGRACER satellites approximated using NRLMSISE00 model.

Copyright © 2023 Advanced Maui Optical and Space Surveillance Technologies Conference (AMOS) – www.amostech.com

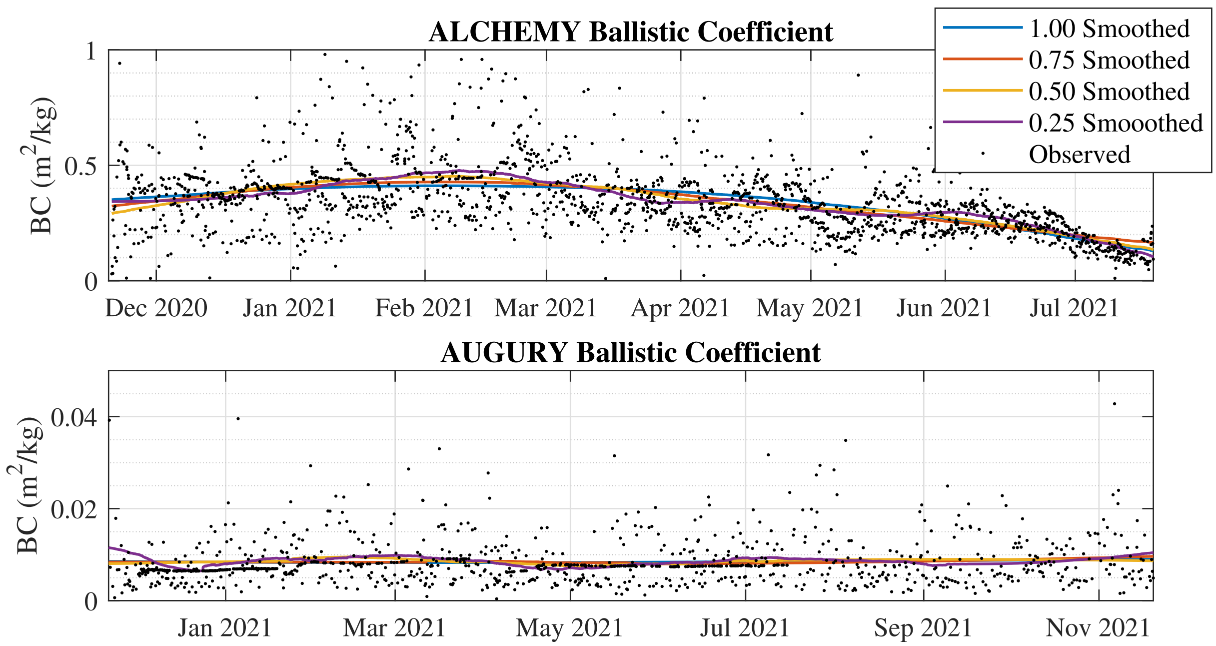

Fig. 8: Ballistic coefficient approximations for DRAGRACER satellites.

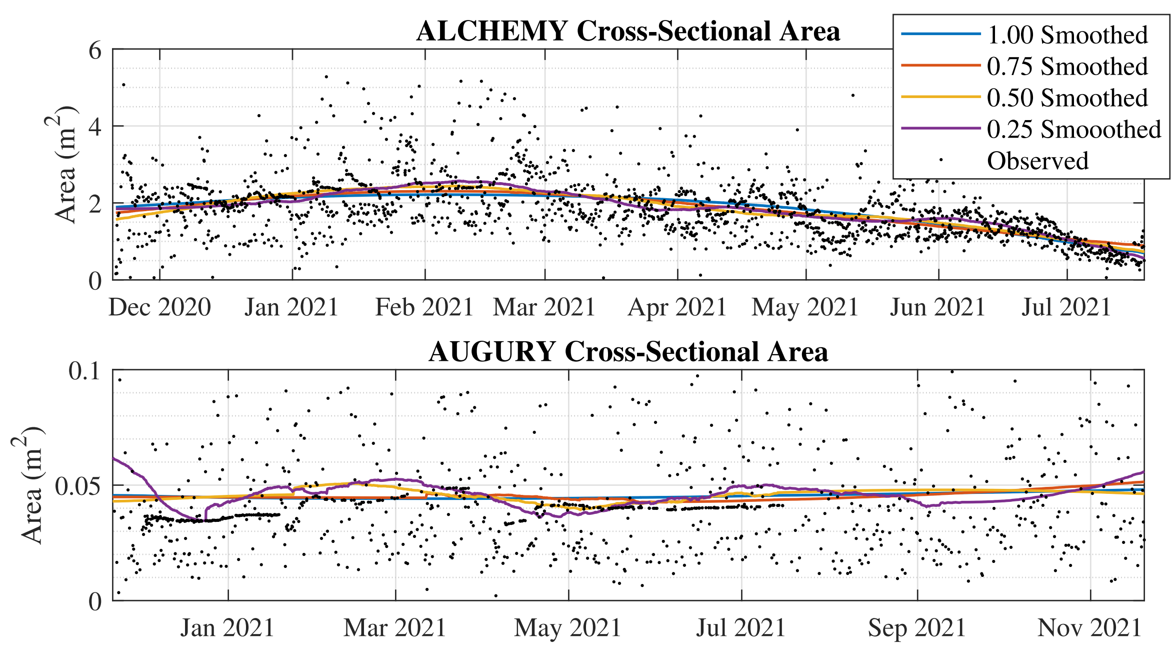

Fig. 9: Effective drag area approximations for DRAGRACER satellites.

Copyright © 2023 Advanced Maui Optical and Space Surveillance Technologies Conference (AMOS) – www.amostech.com

3. RADIOMETRIC STUDY

3.1 Observability Objectives

The radiometric tracking tasks for the DRAGRACER study are aimed at confirming the observability and utility of COTS LEDs on the external surfaces of the spacecraft, observability of the reflective tether, and observability of the satellite main structure, all using a ground-based electro-optical sensor. The COTs LEDs should enable nighttime observability in pure umbra conditions while the LEDs are powered. Lower bound estimates suggest the LEDs would remain powered from the on-board battery packs for approximately 7 days. Solar panels affixed to four external surfaces of each satellite should extend the lifetime beyond 7 days so long as the satellites are exposed to sunight. DRAGRACER terminator observation opportunities for southern California existed between April and July 2021. During this window, sun-glint observations can be collected for both DRAGRACER satellites. The intensity of the ALCHEMY sun-lit datasets is expected to be significantly higher than the LED or main structure intensities.

Prior to launch, a reflection spectrum analysis was performed on each of the satellite's major surface components such as the solar panels, exposed aluminum, exposed printed circuit boards (PCBs), light emitting diodes (LEDs), etcetera. This novel technique was done to better estimate the light reflecting from the spacecraft during terminator passes and optically track the satellites. Over the course of the DRAGRACER mission's orbital operations, both the ALCHEMY and AUGURY satellites were visually tracked with an automated Commercial Off-The-Shelf (COTS) telescope and camera system. The images taken during these tracking operations were later passed through multiple methods of object detection to determine which images had a spacecraft within them for a relative intensity analysis. These methods of optical analysis on satellites bring to light new techniques that could benefit future missions in not only object detection but also satellite-specific discrimination.

3.2 Reflection Spectrum Analysis

Initially, the analysis on the reflection spectrum of the spacecraft's major surface components facilitated selection of the imaging sensor used to track the satellite on orbit. A calibrated spectrometer and light source were directed at each component individually in order to later be combined and determine an average reflection spectrum. It was found that the spacecraft's reflection spectrum was greatest in the near-infrared (NIR) regime surrounding 1550 nm due to the large surface area covered by the solar panels. However, the mission objective of determining the efficacy of the on-board LEDs led to the selection of a visible spectrum sensor with the spectral response shown in Figure 10.

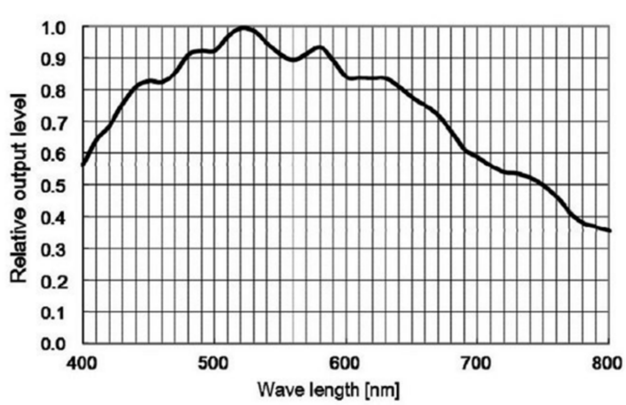

Fig. 10: The relative voltage output of the tracking camera sensor used for DRAGRACER.

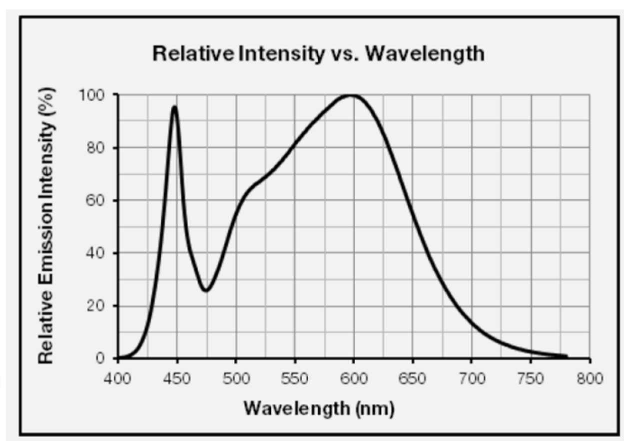

Fig. 11: The emission spectrum of the LEDs on-board the DRAGRACER satellites.

The average reflection spectrum across all surfaces was used as the attitude of the spacecraft would be unknown while on-orbit. Additionally, the drag-tail was assumed to be untwisted again due to the unknown performance on-orbit. Pairing the average spectrum of these surfaces with the LED emission spectrum shown in Figure 11 (and the known

Copyright © 2023 Advanced Maui Optical and Space Surveillance Technologies Conference (AMOS) – www.amostech.com

power of the LEDs), the anticipated received spectrum on the ground over the camera's accepted wavelength range is shown in Figure 12. This analysis showed that the camera is relatively efficient to detect both reflections and the LED emissions simultaneously. Future missions may further study this application as a method of discrimination between satellites based on their reflection or emission spectrum. This method of object detection would require simultaneous imaging with a device such as a hyperspectral camera while tracking with a characterized CMOS sensor.

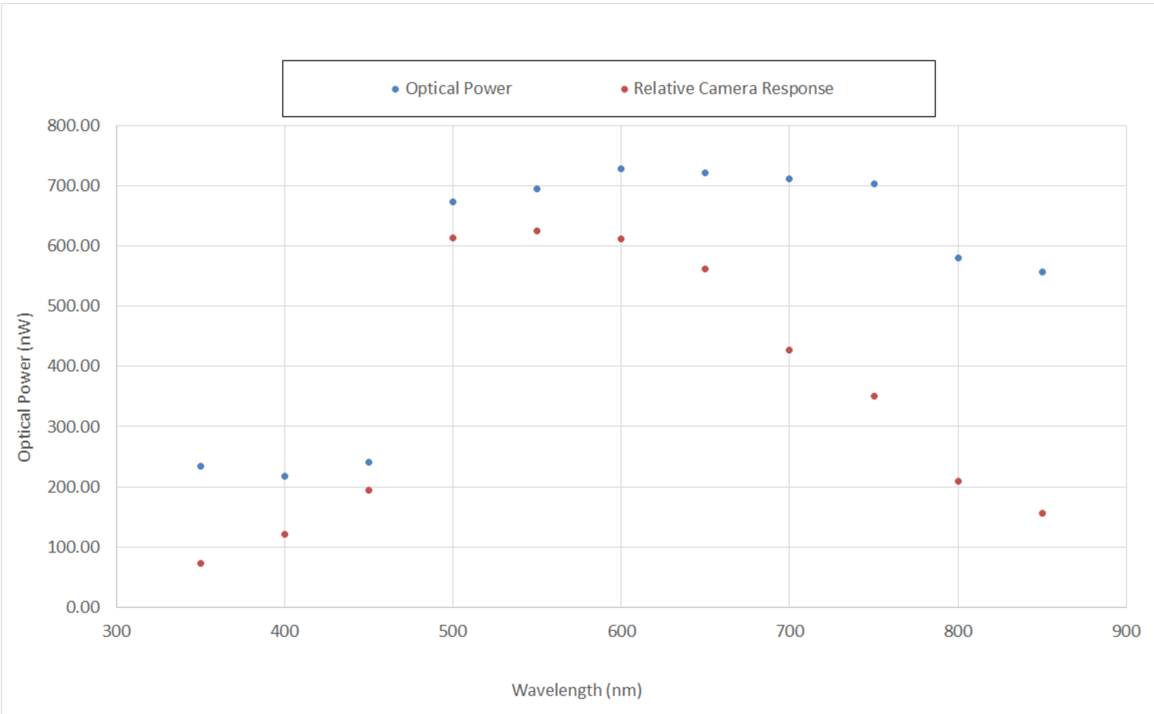

Fig. 12: An overlapping diagram of the anticipated spectrum received on the ground during DRAGRACER tracking activities and the camera's response.

Copyright © 2023 Advanced Maui Optical and Space Surveillance Technologies Conference (AMOS) – www.amostech.com

3.3 Data Collection

DRAGRACER radiometric observations were taken using the mobile optical tracking system outlined in Appendix 4. Data was collected at Millennium Space Systems headquarters in El Segundo, CA (33.916608°N, 118.384131°W) and Joshua Tree, CA (34.266077°N, 116.299094°W). Observation opportunities for the LEDs occurred many times per week while the LEDs were powered. Based on successful data collects, the LEDs were powered for approximately 4 months on-orbit. Example images from LED emmitance is illustrated in Fig. 13. Example images from sun-glint emmitance is illustrated in Fig. 14. Table 4 provides a summary of the data collection dates associated with each attempt to observe DRAGRACER.

Fig. 13: First recorded images of DRAGRACER LEDs. Derived from the 01 December 2020 observation event in El Segundo, CA.

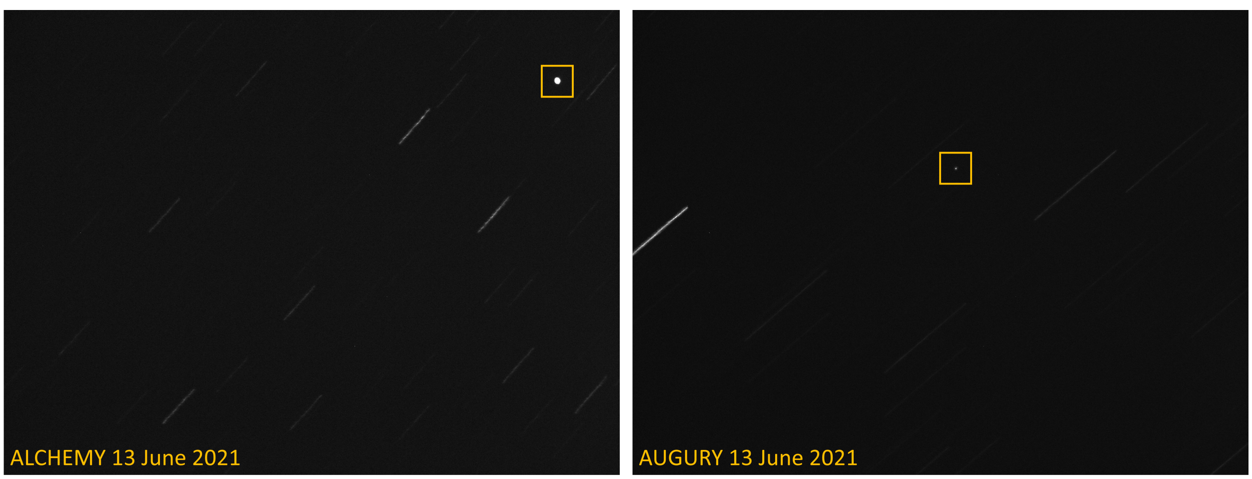

Fig. 14: First recorded images of DRAGRACER sun-glint. Derived from the 13 June 2021 observation event in Joshua Tree, CA.

Copyright © 2023 Advanced Maui Optical and Space Surveillance Technologies Conference (AMOS) – www.amostech.com

Table 4: Observation dates for Millennium ground tracking efforts

Observation Dates	ALCHEMY	AUGURY
01-Dec-2020	✓	✓
02-Dec-2020	✓	
03-Dec-2020	✓	✓
04-Dec-2020		✓
06-Dec-2020		
07-Dec-2020	✓	
12-Dec-2020	✓	
13-Dec-2020		✓
18-Jan-2021	✓	✓
11-Feb-2021		✓
17-Mar-2021	✓	✓
April (unspecified)		
13-Jun-2021*	✓	✓

✓denotes successful data collection event

* denotes sun-glint observations

3.4 Image Analysis

During the post-processing of satellite-tracking images, different object detection techniques were employed to more efficiently gather information pertaining to the satellite itself. Among these are the previously discussed Astropy peak finding algorithm, a match filtering approach used regularly in digital-signal processing, and a convolutional neural network (CNN) approach where an AI was locally trained on a custom data-set made from DRAGRACER images. The latter approach was used in order to determine if there were images containing a spacecraft that the human eye could not discern, with a stretch goal of developing real-time tracking correction capabilities without a human-in-the-loop. The algorithm selected for this purpose was the ”You Only Look Once” (YOLO) method due to its high speed as well as relative accuracy [1]. YOLO and its lightweight variant Fast YOLO have demonstrated object detection rates at 155 frames per second upon release and up to hundreds of frames per second in newer iterations such as YOLOv4 [2]. With the capability of being deployed on small form-factor systems such as a field programmable gate array (FPGA) as well as on modern graphics processing units (GPU), the YOLO algorithm allowed Millennium researchers to quickly train the model on updated datasets and deploy the models to any localized test system in-house. An example of the YOLO detection algorithm running on DRAGRACER data is shown in Fig.15.

Running this algorithm on both the older tracking datasets and the more recent captures, a similar analysis was run to determine relative intensities directly from the FITS files generated from the CMOS tracking camera. By directly analyzing the FITS data rather than the converted PNG images, subjective image adjustments were reduced and the pixel values are directly related to the filling of the CMOS sensor-well a the time of image capture. Similar to previous analysis methods, the peak pixel intensity for the satellite was measured, alongside the average background intensity over the entire image. The difference between these values is recorded, as well as the expected elevation of the specified satellite throughout the overhead pass based on an orbit propagation of the up-to-date two line elements (TLEs). As the latter recorded value was on a separate scale, it was included on a separate axis as shown in the Figure 17. The images in Figure 17 are shown in chronological order to better compare both satellites throughout the mission lifetime.

Copyright © 2023 Advanced Maui Optical and Space Surveillance Technologies Conference (AMOS) – www.amostech.com

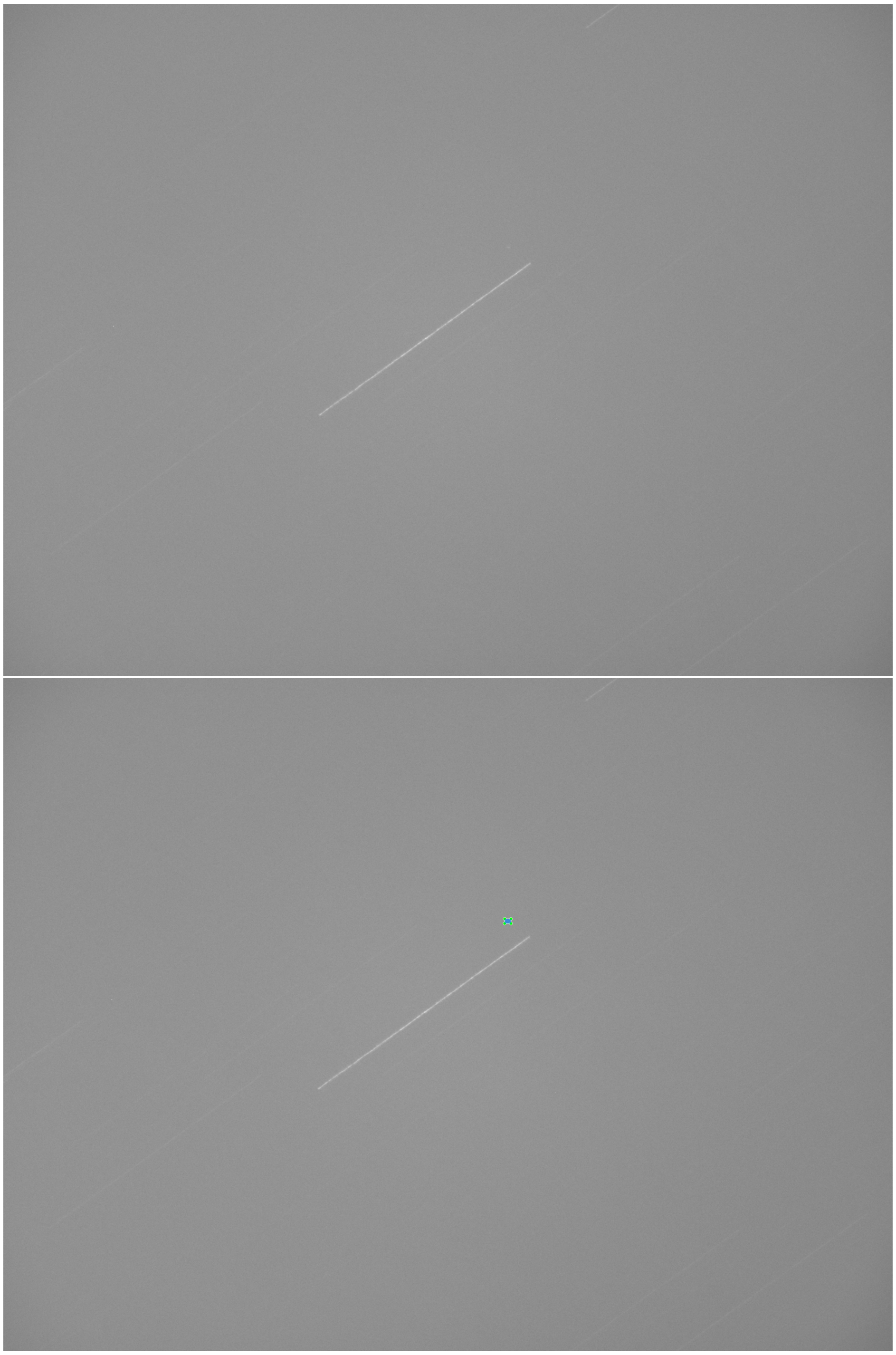

Fig. 15: The YOLO algorithm successfully detecting the ALCHEMY satellite(bottom) from optical tracking data (top).

Copyright © 2023 Advanced Maui Optical and Space Surveillance Technologies Conference (AMOS) – www.amostech.com

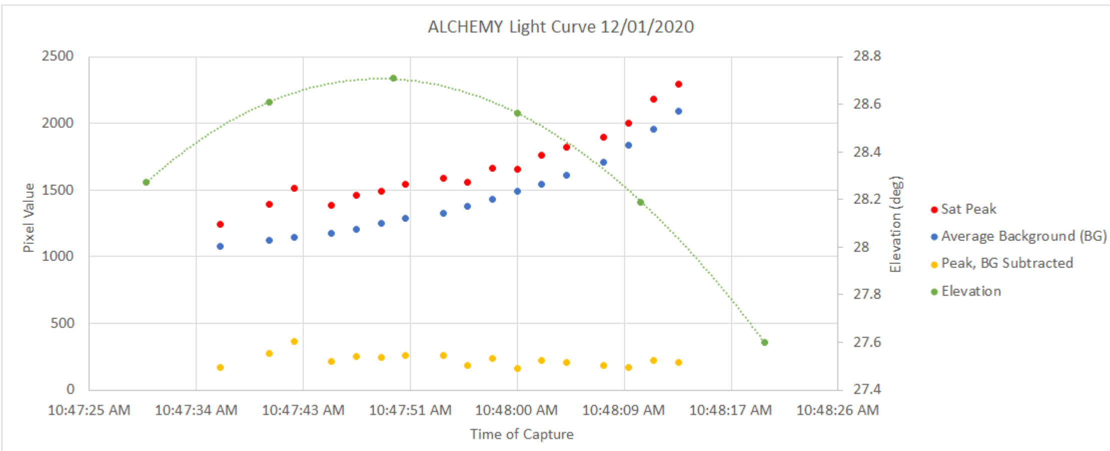

(a)

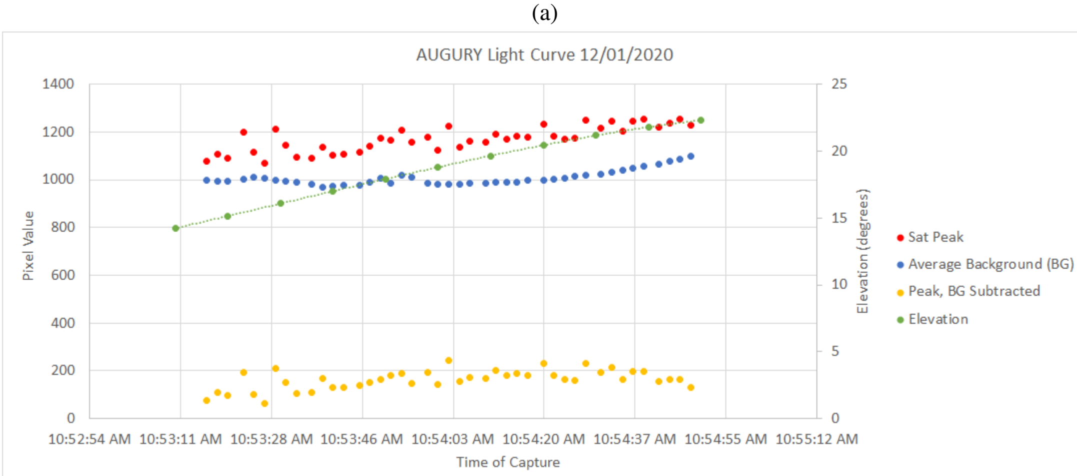

(b)

Copyright © 2023 Advanced Maui Optical and Space Surveillance Technologies Conference (AMOS) – www.amostech.com

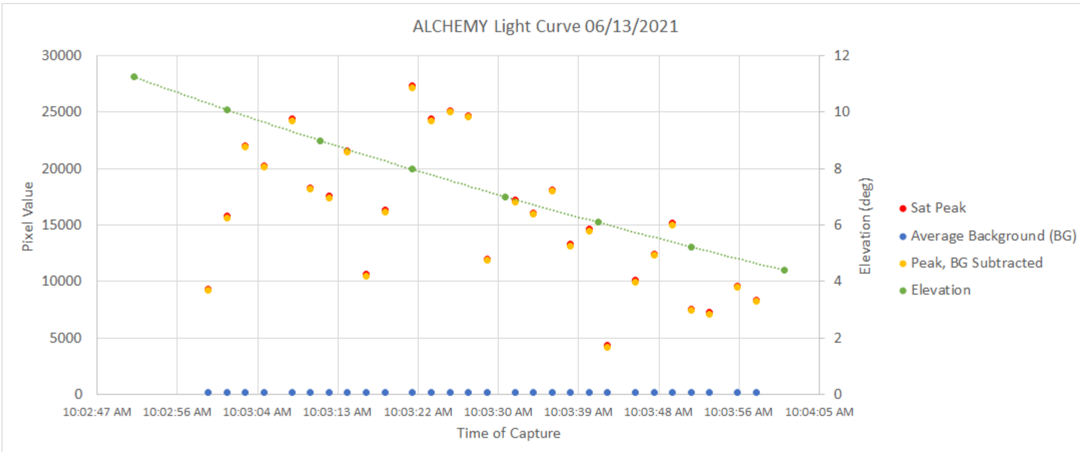

(c)

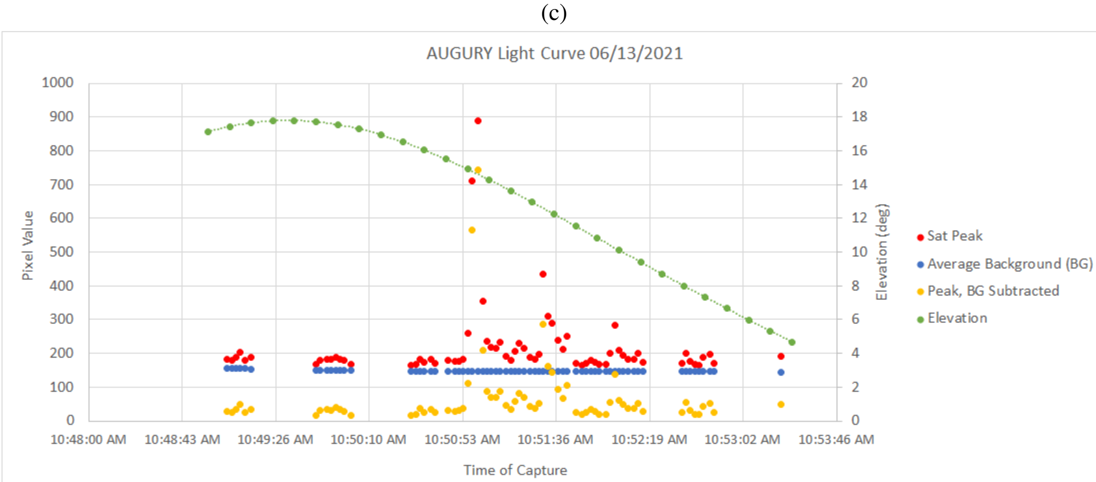

(d)

Fig. 17: An analysis of the relative pixel intensities of the DRAGRACER tracking images with the predicted elevations over the time the overhead pass occurred.

Copyright © 2023 Advanced Maui Optical and Space Surveillance Technologies Conference (AMOS) – www.amostech.com

3.5 Radiometric Study Conclusions

Beginning on the 01 December 2020 pass, a sinusoidal response is seen on the ALCHEMY spacecraft, with the AUGURY spacecraft maintaining a relatively constant intensity. As this is only a singular data-point, only the rotation of the spacecraft may be determined, although it may be noted that the intensity of the ALCHEMY spacecraft seems that it may occur more than 1° after the maximum elevation angle. As the LEDs on-board both spacecraft have a wide divergence angle, it is possible that the amount of time no light is pointing towards the earth is very short and is thus not shown in these data-sets. From this singular pass, it can be inferred that the ALCHEMY spacecraft is rolling such that one LED surface pointed toward the detector roughly every 1.5 minutes and that the AUGURY spacecraft is either not rolling in a well-behaved manner (about the velocity vector) or that it is rolling very quickly (though still not in a well-behaved manner), with potential sinusoidal peaks occurring every 15 to 30 seconds. This is due to the ALCHEMY and AUGURY containing the same LEDs, but the ALCHEMY spacecraft appearing nearly two times brighter. These trends continued throughout the December passes, although with varying success in optically tracking both spacecraft. ALCHEMY continued with a consistent rotation of 0.5° per second and peaks at around 25° to 35° for the majority of the observed passes. AUGURY appears to complete one quarter rotation every minute (1.5° per second) although not in a well-behaved manner, making it difficult to discern from noise.

The data from January and February of 2021 was scarce. It is likely that cloud-cover greatly contributed to the lack of data. The final LED-only scenario pass occurred on 17 March 2021. This pass shows a sinusoidal intensity profile from the AUGURY spacecraft at about half the rate previously seen, although the intensity remains consistently half that of the ALCHEMY spacecraft meaning it is still not rolling about the velocity vector when compared to ALCHEMY. The scarce data from ALCHEMY on this date leaves it difficult to infer any further information about this spacecraft.

On the June 13 pass, the ALCHEMY spacecraft achieved a peak intensity on the order of 25 times greater than the AUGURY spacecraft at approximately half the elevation. The large differences between the ALCHEMY and AUGURY spacecraft, could be contributed to a much larger reflection surface created by the drag tape as both satellites were in terminator conditions. While the ALCHEMY images were too scarce to determine its potential orientation, the AUGURY data-set contained peaks at 30 second increments, adding weight to the December estimates of rotational rate. The drag tape generates large amounts of reflected solar light during terminator operations, increasing optical tracking capabilities of spacecraft with these devices included. With more optical tracking opportunities, it is theorized that it is possible to determine spacecraft rotation rates given on-board optical beacons or ample overhead terminator passes.

4. SUMMARY OF STUDY OUTCOMES

The DRAGRACER flight experiment proved successful on all fronts. Space tether performance was effectively quantified using reported orbit tracking information. Existing and developed deorbit models accuracies were tested against real life data sets and used to help predict the reentry of the AUGURY flight module. Tether dynamics were investigated using two-separate multi-link tether simulations. The observability of the COTS LEDs, reflective tether, and satellite surface were each observed using ground-based electro-optical tracking equipment.

ALCHEMY reentered Earth's inner atmosphere at a significantly faster rate than AUGURY, as expected. Initial estimates over-approximated the efficiency of both the terminator tape and solar activity leading to more accelerated predictions of the DRAGRACER reentry dates. Nonetheless, the data collected suggests ALCHEMY experienced 40 times more exposed surface area than AUGURY, ultimately proving the NSTT about 20% effective against its maximum possible surface area capability, and reducing high-energy collision risks by 96%.

Data collected from Millennium's portable optical tracking station proved that the Samsung COTS LEDs could be used on-orbit. In future applications, the LEDs can be modulated to communicate information to other satellites or Earth-based observers. The tether was indeed highly reflective and provided the highest intensity signals for our detection device (exhibiting enough intensity to be observable by the naked eye!).

Follow-on efforts could include a deeper analysis into the flexible dynamics of the tether to better understand expected deployment behaviors, winding and tangling risks, and how the gravity-gradient and aerodynamic torques interact. Furthermore, an active ED tether demonstration would be an excellent follow-on in order to understand the deorbiting capabilities of ED tethers at higher LEO altitudes where the magnetic field interactions can be of greater use to dive a satellite deeper into regions of higher atmospheric density.

Copyright © 2023 Advanced Maui Optical and Space Surveillance Technologies Conference (AMOS) – www.amostech.com

APPENDIX

Millennium Space Systems Optical Tracking Setup

The Millennium ground optical tracking setup consists of commercially available hardware and software. The camera sensor is a ZWO ASI 1600 MM CMOS camera. The optical telescope assembly (OTA) is a Celestron Rowe-Ackermann Schmidt Astrograph (RASA) with 11 in. aperture. A Software Bisque Paramount MyT equatorial mount is used to track the satellites. TLEs are inputted into TheSkyX Professional tracking software which sends real-time commands to the mount to track moving satellites across the sky. Figures 18-20 illustrate the mobile tracking station equipment. Tables 5-7 provide the technical specifications for the mobile tracking station.

Fig. 18: ZWO ASI 1600 MM Camera

Table 5: Camera sensor specification

ZWO ASI 1600 MM Camera	
Sensor	4/3 in. Panasonic MN34230 CMOS
Diagonal	22.2 mm
Resolution	16.4 MP
Pixel Size	3.8 μm
Full Resolution Frame Rate	23 fps
Read Noise	1.2 e @ 30 db gain

Fig. 19: RASA 11 Optical Telescope Assembly

Table 6: Optical telescope assembly specifications

Celestron Rowe-Ackermann Schmidt Astrograph	
Aperture Diameter	11 in / 279 mm
Focal Length	620 mm
F Number	$f/2.2$
Limiting Magnitude	16

Copyright © 2023 Advanced Maui Optical and Space Surveillance Technologies Conference (AMOS) – www.amostech.com

Fig. 20: Software Bisque Paramount MyT Equatorial Mount

Table 7: Telescope mount specification

Software Bisque Paramount MyT equatorial mount specifications	
Max Slew Speed	6 deg/sec
Object Database	resident space object database (TLE)
Tracking Type	open loop

REFERENCES

[1] Joseph Redmon, Santosh Divvala, Ross Girshick, and Ali Farhadi. You only look once: Unified, real-time object detection, 2016.

[2] Alexey Bochkovskiy, Chien-Yao Wang, and Hong-Yuan Mark Liao. Yolov4: Optimal speed and accuracy of object detection, 2020.

The views, opinions, and/or findings expressed are those of the author(s) and should not be interpreted as representing the official views or policies of the Department of Defense or the U.S. Government

This research was developed with funding from the Defense Advanced Research Projects Agency (DARPA).

Distribution Statement "A" (Approved for Public Release, Distribution Unlimited)

Copyright © 2023 Advanced Maui Optical and Space Surveillance Technologies Conference (AMOS) – www.amostech.com